

Synthetic Polymer Hybridization with DNA and RNA Directs Nanoparticle Loading, Silencing Delivery, and Aptamer Function

Zhun Zhou, Xin Xia, and Dennis Bong*

Department of Chemistry and Biochemistry, The Ohio State University, 100 West 18th Avenue, Columbus, Ohio 43210, United States

S Supporting Information

ABSTRACT: We report herein discrete triplex hybridization of DNA and RNA with polyacrylates. Length-monodisperse triazine-derivatized polymers were prepared on gram-scale by reversible addition–fragmentation chain-transfer polymerization. Despite stereoregio backbone heterogeneity, the triazine polymers bind T/U-rich DNA or RNA with nanomolar affinity upon mixing in a 1:1 ratio, as judged by thermal melts, circular dichroism, gel-shift assays, and fluorescence quenching. We call these polyacrylates “bifacial polymer nucleic acids” (bP_oNAs). Nucleic acid hybridization with bP_oNA enables DNA loading onto polymer nanoparticles, siRNA silencing delivery, and can further serve as an allosteric trigger of RNA aptamer function. Thus, bP_oNAs can serve as tools for both non-covalent bioconjugation and structure–function nucleation. It is anticipated that bP_oNAs will have utility in both bio- and nanotechnology.

The growing importance of nucleic acids in biotechnology¹ and materials² presents a need for well-defined methods to bridge native and artificial architectures. One conceptual approach to this goal involves the synthesis of polymers capable of biomimetic molecular recognition of nucleic acids. Polyacrylate analogues of nucleic acids were first reported in 1966 by Jones,^{3,4} followed by many other alternate backbones,⁵ including polyester, polyvinyl,⁶ and polyamide,⁷ presaging peptide nucleic acid (PNA)⁸ and other nucleic acid backbone replacement studies,⁹ although the hybridization was poorly defined and inefficient.¹⁰ These and other¹¹ polymer nucleic acid analogues require several days of incubation with DNA to yield a hypochromic shift and exhibit a thermal transition. Recent studies using controlled living radical polymerization to produce nucleic acid mimics¹² and hydrogen-bonding polymers have focused on fully artificial assemblies.¹³ Notably, nucleic acid hybridization with length-monodisperse polymers presenting non-native bases has not been studied. We describe herein “bifacial polymer nucleic acids” (bP_oNAs), a family of low-polydispersity polyacrylates that engage T/U oligonucleotide tracts with nanomolar affinity via a synthetic triazine^{14,15} base-triple interface. In contrast to prior efforts to bind polymers to DNA via Watson–Crick base pairing, we find that biomimetic high-affinity, well-defined bP_oNA–DNA triplex hybridization occurs upon mixing, enabling *nonelectrostatic* polymer nanoparticle loading, RNA silencing delivery, and RNA aptamer turn-

on, thus demonstrating the possible applications and functionality of these constructs.

Triaminotriazine (melamine) can recognize thymine/uracil hydrogen-bonding patterns^{16–19} in both organic^{20,21} and aqueous milieu^{13,22–29} and facilitates functional binding to DNA and RNA on a peptide^{30–34} backbone. We hypothesized that polymer-displayed melamine could drive discrete polyacrylate–DNA triplex hybridization (Figure 1) despite regio- and stereochemical heterogeneity in the carbon backbone. Polyacrylates from *tert*-butyl and *N*-hydroxysuccinimidyl (NHS)

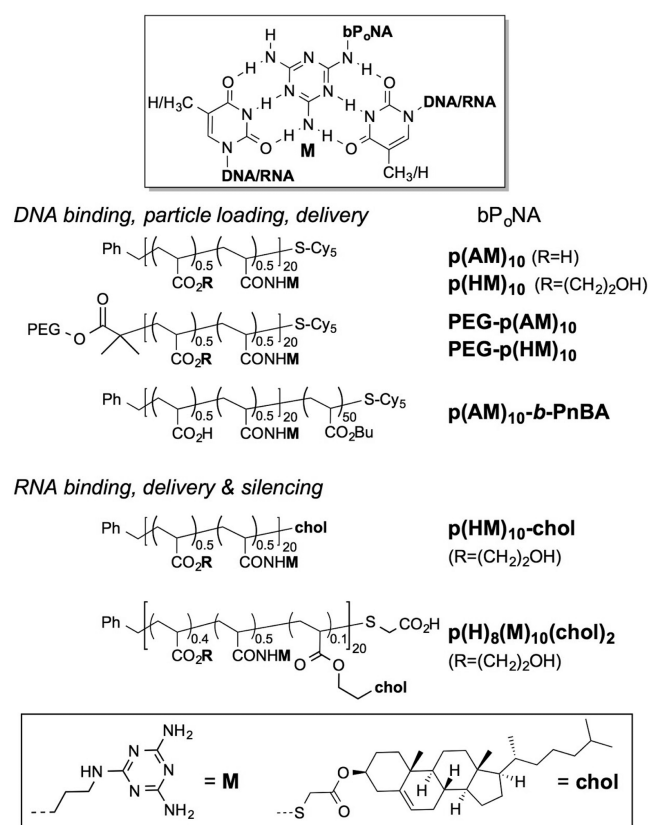


Figure 1. (top) Melamine (M)-driven triplex hybridization of bifacial polymer nucleic acid (bP_oNA) with T/U tracts in DNA and RNA. (bottom) Structures of bP_oNA studied as DNA and RNA folding and delivery agents. PEG = 5 kDa.

Received: May 27, 2015

Published: July 3, 2015

ester monomers were prepared using reversible addition–fragmentation transfer (RAFT) polymerization.³⁵ Amidation of NHS sites with aminoalkyl melamines (M), *tert*-butyl ester cleavage to give the acid (A), and fluorescent end labeling with Cys^{35,36} produced anionic p(AM)₁₀ (Figure 1). Complexation of p(AM)₁₀ to T-rich DNA (dT₁₀C₁₀T₁₀) was reflected in a strong hypochromic shift of the DNA UV absorbance upon mixing. This polymer–DNA complex melted cooperatively at 49 °C (Figure 2). Electrostatic repulsion with DNA was reduced by

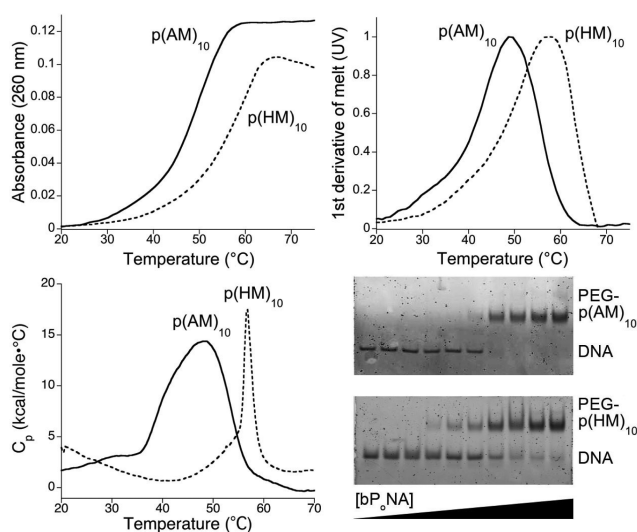


Figure 2. Cooperative and discrete exothermic assembly of bP_oNAs p(AM)₁₀ and p(HM)₁₀ with dT₁₀C₁₀T₁₀ DNA, as indicated by (top left) thermal denaturation curves, (top right) their normalized first derivative curves (UV), and (bottom left) DSC. (bottom right) Native PAGE of dT₁₀C₁₀T₁₀ at a constant concentration with increasing levels of PEG diblock bP_oNA.

replacement of the anionic carboxylate (A) with the neutral 2-hydroxyethyl (H) side chain, yielding bP_oNA p(HM)₁₀. Though the p(HM)₁₀–DNA complex is more thermally stable ($T_m = 59$ °C), differential scanning calorimetry (DSC) analysis revealed that binding of DNA to p(AM)₁₀ was more exothermic (–228 kcal/mol) than to p(HM)₁₀ (–62 kcal/mol). The limited solubility of p(HM)₁₀ complicates deeper analysis. Strongly exothermic assembly³⁷ is consistent with melamine–thymine triplex base stacking.^{30,31} Indeed, loss of three M sites decreased the thermal stability of the polymer–DNA complex by ~10 °C, while a loss of seven M sites completely abolished DNA binding. Similarly, loss of thymine content via T → C substitutions in DNA rapidly degraded polymer complexation (Figures S2–S5 in the Supporting Information). Steric sensitivity was also observed: shortening of the dC₁₀ linker by six nucleotides (dT₁₀C₄T₁₀) resulted in total loss of DNA binding. Furthermore, shortening or lengthening of the polymer side chain by just one CH₂ unit led to an ~8 °C decrease in the thermal stability of the bP_oNA–DNA complexes (Figure S1). In view of the heterogeneity of the bP_oNA backbone, the sensitivity of polyacrylate–DNA complexation to subtle structural perturbations is remarkable and reflects a well-defined molecular interaction governed primarily by the side-chain environment.

The (AM)₁₀ and (HM)₁₀ DNA complexes did not survive native polyacrylamide gel electrophoresis (PAGE), possibly because of nonspecific interactions with the gel. Sterically protected⁴³ polymers (Figure 1) were prepared using a poly(ethylene glycol) (PEG)-derivatized chain-transfer agent.⁴⁴

The resulting [PEG-bP_oNA]–DNA complexes could be observed on gel, reflective of defined polymer–DNA hybridization (Figure 2). Discrete two-state complexation was further indicated by an isodichroic point (237 nm) in the circular dichroism (CD) spectra of dT₁₀C₁₀T₁₀ upon titration with p(AM)₁₀, amid inversion of a positive CD band at 277 nm into a negative signal at 260 nm and a positive absorption at 220 nm (Figure 3). The polymer itself exhibits negligible CD under these

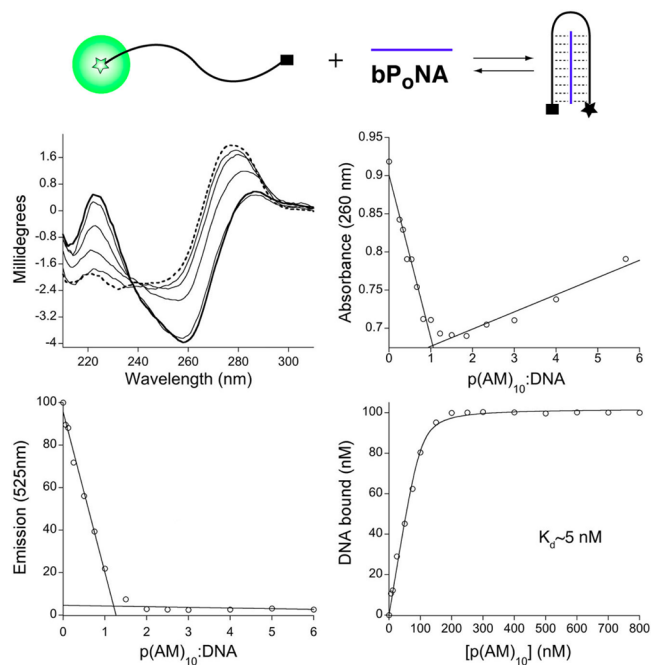


Figure 3. Titration of p(AM)₁₀ with dT₁₀C₁₀T₁₀. (middle left) Change in free DNA CD (---) upon treatment with increasing p(AM)₁₀ (—). (middle right) Job plot from UV absorbance. (bottom left) Job plot from fluorescence quenching using DNA with terminal fluorophore and quencher, as illustrated at in the scheme at the top. (bottom right) Fluorescence quenching isotherm fit to a 1:1 binding model (—).

conditions. Binding of p(AM)₁₀ with a dT₁₀C₁₀T₁₀ DNA that was 3'- and 5'-derivatized with dabcyf and fluorescein resulted in full fluorescein quenching at a 1:1 ratio, thus providing support for the triplex hairpin binding model. This binding ratio was corroborated by a UV Job plot. Furthermore, fluorescence quenching and anisotropy curves fit well to a 1:1 binding model, yielding $K_d = 2–5$ nM (Figure 3). These data, together with the DSC results, indicate high-affinity enthalpically driven bP_oNA–DNA triplex hybridization.

The functional compatibility of polymer hybrid triplex stems with aptamer folds was studied using a mutant of the RNA aptamer Spinach,³⁸ which can capture a fluorogenic small molecule, 3,5-difluoro-4-hydroxybenzylidene imidazolone (DFHBI), within a G-quadruplex binding pocket,^{39,40} eliciting green emission. Replacement of stem P2 with an unstructured U₁₀CACAU₁₀ loop, as in U-Spinach, ablates DFHBI binding and fluorescence; bifacial PNA (bPNA) can fold the U-loop into a triplex hybrid P2 stem and restore ~30% of the DFHBI emission intensity in the peptide–RNA hybrid complex.³³ Strikingly, the polymer analogues p(AM)₁₀, PEG-p(AM)₁₀, and PEG-p(HM)₁₀ can rescue aptamer function in U-Spinach with greater efficiency than the peptide (Figure 4), with excitation and emission intensities closer to those of the binary Spinach–DFHBI complex. Furthermore, the polymer–RNA hybrids activate

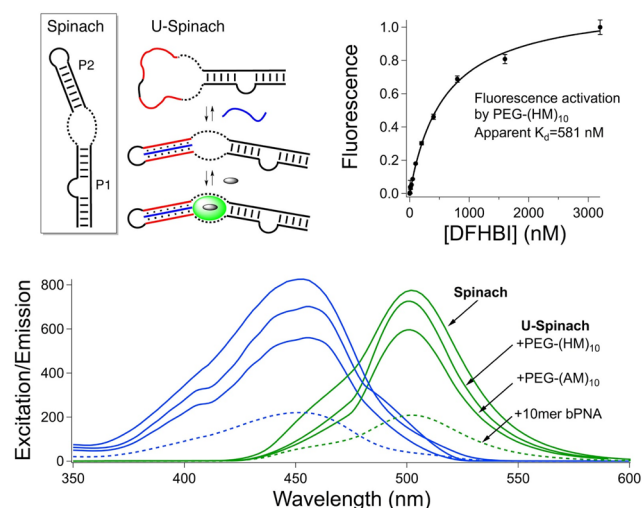


Figure 4. Aptamer turn-on by bifacial polymer nucleic acid. (top left) Spinach aptamer fold, with the fluorogen binding site shown as a dashed line; refolding of U-Spinach by bP₀NA (blue) and DFHBI binding, with U tracts shown in red. For clarity, the PEG block is not indicated. (top right) Fluorescence activation of DFHBI by the bP₀NA-U-Spinach binary complex, fit to a 1:1 binding model. (bottom) Excitation (blue) and emission (green) spectra for the indicated DFHBI complexes. The excitation and emission intensities follow the same trend.

DFHBI fluorescence with apparent K_d values of ~0.5 μM, similar to Spinach. The neutral PEG-(HM)₁₀ is the most efficient fluorescence trigger, reflective of enhanced affinity over the negatively charged p(AM)₁₀ polymers. The functional compatibility of PEG diblock bP₀NA hybrid stems with folded RNA elements is likely to be general;³³ bP₀NA could thus be useful for non-covalent conjugation of aptamer modules with polymer carrier platforms for targeted delivery.^{41,42}

We set out to test the extent to which bP₀NA could be used to connect nucleic acids to other synthetic architectures useful for delivery, such as polymer nanoparticles and lipids. The diblock polyacrylate amphiphile p(AM)₁₀-b-PnBA (Figure 1) was constructed and found to form ~300 nm particles in PBS. Addition of dT₁₀C₁₀T₁₀ spontaneously dispersed the polymer assembly into ~20 nm particles that remained stable over days in buffer, as judged by dynamic light scattering (DLS) and ambient transmission electron microscopy (TEM) (Figure 5). These data support binding of DNA to bP₀NA strands on the particle surface, leading to dispersion through increased electrostatic repulsion. Sedimentation studies revealed that up to 62% of solution DNA could be cosedimented with polymer depending on the DNA thymine content (Table S3). These DNA-loaded particles were readily taken up by HEK-293 and MCF-7 cells in culture (Figure S14), indicating robust conjugation of DNA to diblock bP₀NA nanoparticles. We probed the utility of bP₀NA nanoparticles as vehicles for siRNA knockdown in HeLa cells stably expressing firefly and renilla luciferase.⁴⁵ However, although an optimized⁴⁶ sense/antisense RNA duplex targeted to firefly luciferase could be loaded onto diblock bP₀NA nanoparticles via 3'- and 5'-terminal rU₁₀ tracts, no silencing activity was observed.

Binding to the siRNA duplex by sterol-derivatized bP₀NA was confirmed by the emergence of a new melting transition at ~65 °C, representing the triplex hybrid domain (Figure S7). We therefore speculated that inefficient RNA release from the nanoparticle was preventing silencing. We prepared instead bP₀NA hybrids for non-covalent lipidation of U-tract siRNA

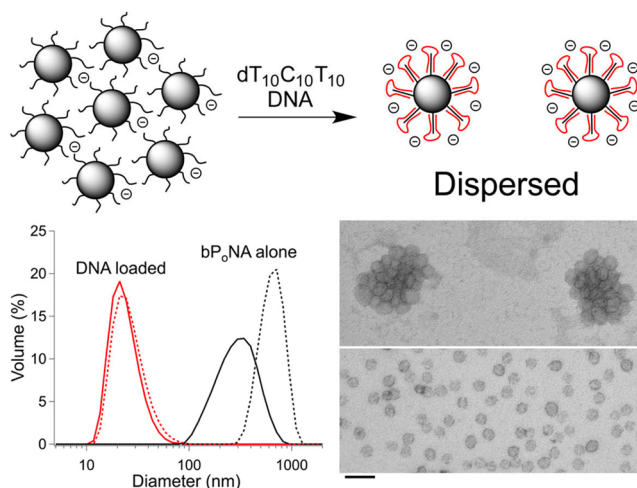


Figure 5. (top) Aggregated bP₀NA nanoparticles disperse upon binding of DNA (red). (bottom left) DLS of p(AM)₁₀-b-PnBA nanoparticles with (red) and without (black) DNA loading after 6 h (—) and 72 h (---). (bottom right) TEM images of uranyl acetate-stained particles clustered without DNA and dispersed after DNA binding. The scale bar is 100 nm.

duplexes, which was expected to facilitate silencing.⁴⁷ The cholesterol-modified bP₀NAs p(HM)₁₀-chol and p(H)₈(M)₁₀(chol)₂ (Figure 1) were synthesized to achieve duplex lipidation either via polymer end (p(HM)₁₀-chol) or brush (p(H)₈(M)₁₀(chol)₂) functionalization. Gratifyingly, dose-dependent knockdown of up to 40% luciferase silencing was observed using both of these charge-neutral carriers, similar to that observed⁴⁷ with covalent siRNA lipidation (Figure 6).

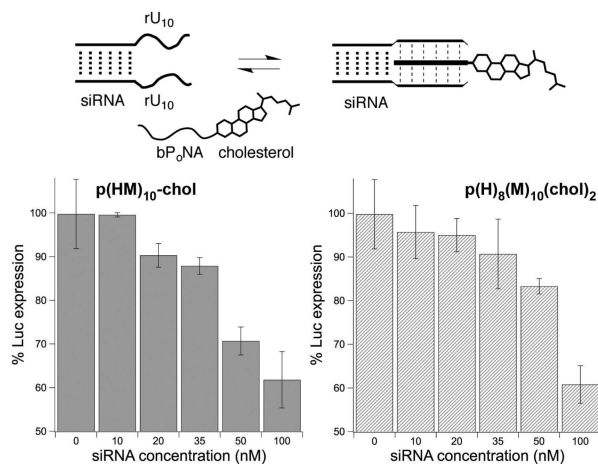


Figure 6. (top) Concept of non-covalent siRNA lipidation with bP₀NA-chol. (bottom) Luciferase silencing in HeLa-Luc cells upon delivery of siRNA at optimized polymer:RNA ratios of 5:1 and 10:1 using (left) p(HM)₁₀-chol and (right) p(H)₈(M)₁₀(chol)₂ as polymer carriers.

Notably, the same U-tract siRNA duplex can be functionalized with different bP₀NA carriers, enabling facile evaluation of lipid polymers without preparation of new RNA derivatives. Thus, nucleic acid loading and delivery functions can be integrated into a single (neutral) polymer synthesis without covalent nucleic acid modification^{48,49} or the use of cationic components. This affords greater control over charge tuning in nucleic acid delivery systems.^{50,51}

Taken together, these studies describe discrete, well-defined, and predictable triplex hybridization of T/U-rich DNA and RNA with bifacial polymer nucleic acids (bP_oNAs). Unlike peptide synthesis or biological expression, the products of radical copolymerization are structurally diverse as a result of uncontrolled stereochemistry and monomer distribution. Despite this heterogeneity, triazine–thymine docking decisively drives assembly, eliciting recognition properties reminiscent of rigorously defined chemical entities. Rapid, biomimetic DNA/RNA docking on the abiotic triazine base-triple interface sets bP_oNA apart from prior studies on polymer-displayed native nucleobases. bP_oNAs thus provide access to discrete molecular binding motifs of T/U-rich DNA and RNA using polymer synthesis from cheaply available starting monomers. This scalable and well-defined assembly strategy enables seamless integration of polymer architectures with DNA and RNA and their use in aptamer turn-on, delivery, and siRNA silencing. We anticipate that bP_oNAs may be tuned at the monomer level to accommodate a wide range of bio- and nanotechnology applications.

■ ASSOCIATED CONTENT

Supporting Information

Detailed experimental procedures and additional data. The Supporting Information is available free of charge on the ACS Publications website at DOI: 10.1021/jacs.5b05481.

■ AUTHOR INFORMATION

Corresponding Author

*bong.6@osu.edu

Notes

The authors declare no competing financial interest.

■ ACKNOWLEDGMENTS

This research was supported in part by NSF-DMR and NIH. We are grateful to Alnylam Pharmaceuticals for sharing the dual-luciferase HeLa cell line.

■ REFERENCES

- (1) Burnett, J. C.; Rossi, J. J. *Chem. Biol.* **2012**, *19*, 60.
- (2) Roh, Y. H.; Ruiz, R. C. H.; Peng, S.; Lee, J. B.; Luo, D. *Chem. Soc. Rev.* **2011**, *40* (12), 5730.
- (3) Jones, A. S.; Taylor, N. *Nature* **1967**, *215*, 505.
- (4) Cassidy, F.; Jones, A. S. *Eur. Polym. J.* **1966**, *2*, 319.
- (5) Jones, A. S. *Int. J. Biol. Macromol.* **1979**, *1*, 194.
- (6) Boguslawski, S.; Olson, P. E.; Mertes, M. P. *Biochemistry* **1976**, *15*, 3536.
- (7) Gait, M. J.; Jones, A. S.; Jones, M. D.; Shepherd, M. J.; Walker, R. T. *J. Chem. Soc., Perkin Trans. 1* **1979**, 1389.
- (8) Nielsen, P. E. *Acc. Chem. Res.* **1999**, *32*, 624.
- (9) Eschenmoser, A. *Science* **1999**, *284*, 2118.
- (10) Kaye, H. *J. Am. Chem. Soc.* **1970**, *92*, 5777.
- (11) Lo, P. K.; Sleiman, H. F. *Macromolecules* **2008**, *41*, 5590.
- (12) McHale, R.; O'Reilly, R. K. *Macromolecules* **2012**, *45*, 7665.
- (13) De Greef, T. F. A.; Smulders, M. M. J.; Wolfs, M.; Schenning, A.; Sijbesma, R. P.; Meijer, E. W. *Chem. Rev.* **2009**, *109*, 5687.
- (14) Mittapalli, G. K.; Reddy, K. R.; Xiong, H.; Munoz, O.; Han, B.; De Riccardis, F.; Krishnamurthy, R.; Eschenmoser, A. *Angew. Chem., Int. Ed.* **2007**, *46*, 2470.
- (15) Vysabhattar, R.; Ganesh, K. N. *Tetrahedron Lett.* **2008**, *49*, 1314.
- (16) Lange, R. F. M.; Beijer, F. H.; Sijbesma, R. P.; Hooft, R. W. W.; Kooijman, H.; Spek, A. L.; Kroon, J.; Meijer, E. W. *Angew. Chem., Int. Ed. Engl.* **1997**, *36*, 969.
- (17) Zhou, Z.; Bong, D. *Langmuir* **2013**, *29*, 144.
- (18) Thomas, R.; Kulkarni, G. U. *Beilstein J. Org. Chem.* **2007**, *3*, 17.

- (19) Arambula, J. F.; Ramisetty, S. R.; Baranger, A. M.; Zimmerman, S. C. *Proc. Natl. Acad. Sci. U. S. A.* **2009**, *106*, 16068.
- (20) Whitesides, G. M.; Simanek, E. E.; Mathias, J. P.; Seto, C. T.; Chin, D.; Mammen, M.; Gordon, D. M. *Acc. Chem. Res.* **1995**, *28*, 37.
- (21) Prins, L. J.; Reinhoudt, D. N.; Timmerman, P. *Angew. Chem., Int. Ed.* **2001**, *40*, 2382.
- (22) Kawasaki, T.; Tokuhira, M.; Kimizuka, N.; Kunitake, T. *J. Am. Chem. Soc.* **2001**, *123*, 6792.
- (23) Ariga, K.; Kunitake, T. *Acc. Chem. Res.* **1998**, *31*, 371.
- (24) Ma, M.; Paredes, A.; Bong, D. *J. Am. Chem. Soc.* **2008**, *130*, 14456.
- (25) Ma, M.; Gong, Y.; Bong, D. *J. Am. Chem. Soc.* **2009**, *131*, 16919.
- (26) Ma, M.; Bong, D. *Acc. Chem. Res.* **2013**, *46*, 2988.
- (27) Ma, M.; Bong, D. *Org. Biomol. Chem.* **2011**, *9*, 7296.
- (28) Ma, M.; Bong, D. *Langmuir* **2011**, *27*, 8841.
- (29) Ma, M.; Bong, D. *Langmuir* **2011**, *27*, 1480.
- (30) Zeng, Y.; Pratumyot, Y.; Piao, X.; Bong, D. *J. Am. Chem. Soc.* **2012**, *134*, 832.
- (31) Piao, X.; Xia, X.; Bong, D. *Biochemistry* **2013**, *52*, 6313.
- (32) Xia, X.; Piao, X.; Fredrick, K.; Bong, D. *ChemBioChem* **2014**, *15*, 31.
- (33) Xia, X.; Piao, X.; Bong, D. *J. Am. Chem. Soc.* **2014**, *136*, 7265.
- (34) Piao, X.; Xia, X.; Mao, J.; Bong, D. *J. Am. Chem. Soc.* **2015**, *137*, 3751.
- (35) Keddie, D. J.; Moad, G.; Rizzardo, E.; Thang, S. H. *Macromolecules* **2012**, *45*, 5321.
- (36) Bandyopadhyay, S.; Xia, X.; Maiseiyev, A.; Mihai, G.; Rajagopalan, S.; Bong, D. *Macromolecules* **2012**, *45*, 6766.
- (37) SantaLucia, J., Jr.; Hicks, D. *Annu. Rev. Biophys. Biomol. Struct.* **2004**, *33*, 415.
- (38) Paige, J. S.; Wu, K. Y.; Jaffrey, S. R. *Science* **2011**, *333*, 642.
- (39) Huang, H.; Suslov, N. B.; Li, N.-S.; Shelke, S. A.; Evans, M. E.; Koldobskaya, Y.; Rice, P. A.; Piccirilli, J. A. *Nat. Chem. Biol.* **2014**, *10*, 686.
- (40) Warner, K. D.; Chen, M. C.; Song, W.; Strack, R. L.; Thorn, A.; Jaffrey, S. R.; Ferré-D'Amaré, A. R. *Nat. Struct. Mol. Biol.* **2014**, *21*, 658.
- (41) Oh, S. S.; Lee, B. F.; Leibfarth, F. A.; Eisenstein, M.; Robb, M. J.; Lynd, N. A.; Hawker, C. J.; Soh, H. T. *J. Am. Chem. Soc.* **2014**, *136*, 15010.
- (42) Farokhzad, O. C.; Karp, J. M.; Langer, R. *Expert Opin. Drug Delivery* **2006**, *3*, 311.
- (43) Immordino, M. L.; Dosio, F.; Cattel, L. *Int. J. Nanomed.* **2006**, *1*, 297.
- (44) Bartels, J. W.; Cauet, S. I.; Billings, P. L.; Lin, L. Y.; Zhu, J.; Fidge, C.; Pochan, D. J.; Wooley, K. L. *Macromolecules* **2010**, *43*, 7128.
- (45) Akinc, A.; Zumbuehl, A.; Goldberg, M.; Leshchiner, E. S.; Busini, V.; Hossain, N.; Bacallado, S. A.; Nguyen, D. N.; Fuller, J.; Alvarez, R.; Borodovsky, A.; Borland, T.; Constien, R.; de Fougères, A.; Dorkin, J. R.; Narayanannair Jayaprakash, K.; Jayaraman, M.; John, M.; Koteliansky, V.; Manoharan, M.; Nechev, L.; Qin, J.; Racie, T.; Raitcheva, D.; Rajeev, K. G.; Sah, D. W. Y.; Soutschek, J.; Toudjarska, I.; Vornlocher, H.-P.; Zimmermann, T. S.; Langer, R.; Anderson, D. G. *Nat. Biotechnol.* **2008**, *26*, 561.
- (46) Park, J.-E.; Heo, I.; Tian, Y.; Simanshu, D. K.; Chang, H.; Jee, D.; Patel, D. J.; Kim, V. N. *Nature* **2011**, *475*, 201.
- (47) Soutschek, J.; Akinc, A.; Bramlage, B.; Charisse, K.; Constien, R.; Donoghue, M.; Elbashir, S.; Geick, A.; Hadwiger, P.; Harborth, J.; John, M.; Kesavan, V.; Lavine, G.; Pandey, R. K.; Racie, T.; Rajeev, K. G.; Röhl, I.; Toudjarska, I.; Wang, G.; Wuschko, S.; Bumcrot, D.; Koteliansky, D.; Limmer, S.; Manoharan, M.; Vornlocher, H.-P. *Nature* **2004**, *432*, 173.
- (48) Peterson, A. M.; Heemstra, J. M. *Wiley Interdiscip. Rev. Nanomed. Nanobiotechnol.* **2015**, *7*, 282.
- (49) Kedracki, D.; Chekini, M.; Maroni, P.; Schlaad, H.; Nardin, C. *Biomacromolecules* **2014**, *15*, 3375.
- (50) Nguyen, J.; Szoka, F. C. *Acc. Chem. Res.* **2012**, *45*, 1153.
- (51) Grijalvo, S.; Aviñó, A.; Eritja, R. *Expert Opin. Ther. Pat.* **2014**, *24*, 801.